Experimental Prediction and Design of Ultra-Wideband Raman Amplifiers Using Neural Networks

Xiaoyan Ye, Aymeric Arnould, Amirhossein Ghazisaeidi, Dylan Le Gac and Jeremie Renaudier
Nokia Bell Labs, Paris-Saclay, France (aymeric.arnould@nokia.com)

Abstract: A machine learning method for Raman gain prediction and multi-pump broadband amplifier design is experimentally demonstrated over a 100 nm-wide optical bandwidth. We show high accuracy and ultra-fast prediction of arbitrary gain profile over a 100 km-long SSMF span.
OCIS codes: (060.2330) Fiber optics communications; (060.2360) Fiber optics links and subsystems

1. Introduction

After years of extensive research in coherent transmission technologies to maximize the spectral efficiency in long-haul optical transport, ultra-wideband (UWB) schemes are currently gaining interest as a promising approach to extend the throughput of transmission systems [1-4]. Various solutions have been proposed to achieve UWB amplification, some of them with hybrid configurations using backward Raman pumping combined with either erbium-doped fiber amplifiers (EDFA) [3] or semiconductor optical amplifiers (SOA) [1,4] to improve end of link optical signal to noise ratio. To correctly predict the Raman gain in the hybrid amplification schemes, several methods have been proposed. Although the gain of forward or backward Raman pumping can be predicted by solving a system of nonlinear ordinary differential equations governing the evolution of power profile during the propagation [5], this method is time-consuming and complex as the spectrum bandwidth extends beyond 10 THz and the number of pumps is increased. Machine-learning (ML) techniques have been recently proposed to achieve low-complexity methods to predict the Raman gain, exploiting training data sets coming from numerical simulations [6-8] or experimental measurements [9] over extended C+L systems.

In this paper, we present our ML prediction method for UWB Raman amplifier design, based on an extensive experimental dataset, over a testbed using hybrid Raman SOA amplifier, with 100 nm S+C+L UWB spectrum and 5 Raman pumps between 1410 and 1510 nm [4]. First we demonstrate the ability to use artificial neural networks (ANN) to predict the overall loss profile mixing fiber attenuation, inter-channel stimulated Raman scattering (SRS) and backward pumping, for any pump power configuration. Then, we use an ANN to design the UWB Raman amplifier, by providing the required pump currents to realize a pre-determined loss profile and experimentally validate our method.

2. Machine learning models for Raman amplifier design

Our experimental setup is depicted in Fig. 1a. We used three different amplified spontaneous emission (ASE) noise sources and an UWB wavelength selective switch (WSS) to generate a 100 nm continuous spectrum, spreading from 1515 to 1615 nm. This spectrum was amplified by an UWB SOA before being sent to the fiber under test, which is a 100 km standard single mode fiber (SSMF) span and we used backward fiber Raman amplification with 5 pumps per polarization located at 1410, 1435, 1455, 1490, and 1510 nm. We use a 99/1 coupler, an optical switch and an optical spectrum analyzer (OSA) to obtain the UWB power spectrum at the span input. At the span output, the UWB signal was sent directly to the switch and the OSA. Input and output calibrated spectra are respectively shown in black and grey line in the top right inset of Fig. 1a. We define the span loss profile $\{L_1, \dots, L_m\}$ as the difference between those power profiles, as represented in the bottom right inset of Fig. 1a. This loss profile accounts for the backward Raman pumping contribution which depends on the values of the 5 pump currents $\{I_1, \dots, I_5\}$ (we set the same current on both polarizations for each wavelength), but also for the fiber attenuation and the stimulated Raman scattering (SRS) occurring in high power UWB transmission, that can show a tilt exceeding 4 dB on such a 100 nm bandwidth [4]. In this work, we operated the SOA to provide at the fiber input a 21 dBm optical spectrum with a 6 dB tilt over the bandwidth, to meet the operation conditions of our previous transmission experiment [4]. We then randomly and independently chose the values of each of the pump currents $\{I_1, \dots, I_5\}$ from the uniform distribution $U([200{,}1500]mA)$ and measured 10000 random configurations. The data set has been arbitrarily split into 80% and 20% for training and validation respectively.

To model the system under test, the two ML models that we consider are represented in Fig. 1b. The first one is built to predict the loss profile $\{L_1, \dots, L_m\}$, when we feed the pump currents $\{I_1, \dots, I_5\}$ as an input. This *generative model* allows us first to reproduce the observation of our experiments, and later to predict the loss profile corresponding to unobserved pump current configurations. The second model is an *inverse model*: given a loss profile

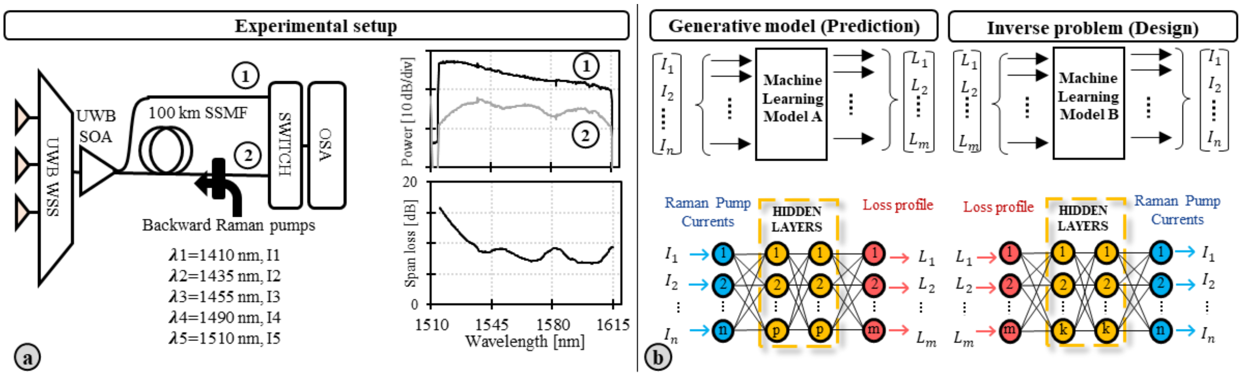

Fig. 1. (a) Single span characterization setup with 5 pumps Raman amplifier and SOA: span input and output power profiles are measured with the OSA (respectively labelled 1 and 2 in top inset) and span loss profile (bottom inset) is deduced. (b) ML models and artificial neural networks (ANN) architectures for span loss profile prediction (model A) and pump current value prediction (model B)

$\{L_1, \ldots, L_m\}$, the model is used to predict the pump currents $\{I_1, \ldots, I_5\}$ to be applied. This model will be useful for transmission line design, since we can use it to set the pump currents to reach a target loss profile. The bottom part of Fig. 1b represents the two multi-layer ANNs we consider in this paper. The ANN for the *generative model* (prediction) is composed of an input layer with $n = 5$ neurons (corresponding to the number of Raman pump currents used in the experiment), an output layer with $m = 100$ neurons (to compute the loss profile) and 2 hidden layers with $p = 150$ neurons. The ANN architecture for model the *inverse problem* (design) is composed of an input layer with m neurons, an output layer with n neurons and 2 hidden layers with $k = 300$ neurons. The activation function was selected to be rectified linear unit (ReLU) for the hidden layers and linear for the output layer.

3. Prediction results and discussion

After the training stage with 8000 files, to evaluate the performance of our ANNs, we use the validation set containing the remaining 2000 files that were unused during the training. First, for the generative model, for each pump configuration of the validation set, we predict the loss profile with the ANN. Fig. 2a shows the prediction error distribution for 10 wavelengths in the spectrum: the ends of the whiskers indicate the 5th and 95th percentiles of the population, the box captures the half population between the 1st and 3rd quartiles, and the horizontal line inside the box indicates the population median. Outside cross markers correspond to predictions that are considered as outliers. We observe that for all wavelengths, the median error does not exceed ±0.2 dB, and that 90% of the validation set show prediction error less than ±0.6 dB. Fig. 2b shows the probability density function (PDF) and cumulative density function (CDF) of the root mean square error (RMSE) between the initial measured profile and the predicted loss over the whole validation set. The mean value of RMSE is 0.25 dB. Besides, the CDF indicates that 95% of the predictions give RMSE less than 0.51 dB. We plot in Fig. 2c the true spectrum (solid line) and the prediction of our ANN (diamond markers), for the best fit with a RMSE of 0.099 dB and for the case corresponding to the 95th RMSE percentile, i.e. with RMSE = 0.51 dB. This figure clearly illustrates the high accuracy of the prediction for our 100 nm-wide optical signal.

Then, for the inverse model, for each measurement in the validation data set, we feed the loss profile as the input of the ANN and we predict the corresponding pump current configuration. To assess the performance of our ANN, we first show in Fig. 3a the relative current errors for the whole validation set: the prediction error for the 5 currents $\{I_1, \ldots, I_5\}$ is less than ±13% for 90% of the cases. Then, for the 2000 files of the validation data set, we use the predicted currents in our experimental testbed and re-measure the obtained loss to observe the impact of current

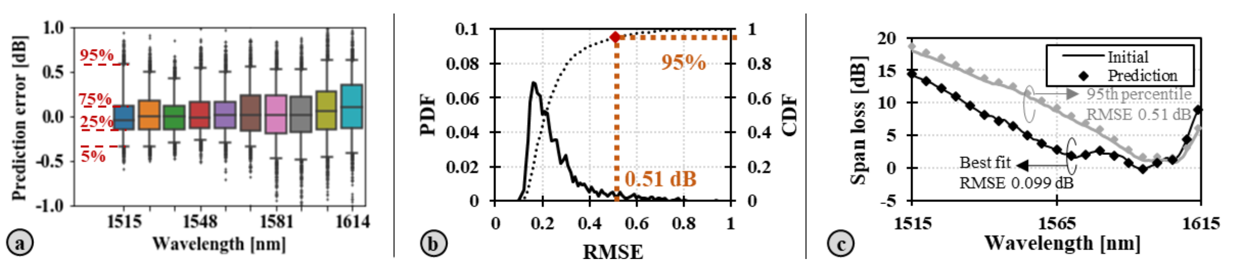

Fig. 2. Generative model prediction results. (a): loss profile prediction error repartition for 10 wavelengths in the UWB spectrum; (b): probability density function (PDF) of the RMSE and cumulative density function (CDF) of the RMSE of the prediction error; (c): initial spectrum and predicted profile for the best case and the 95th RMSE percentile.

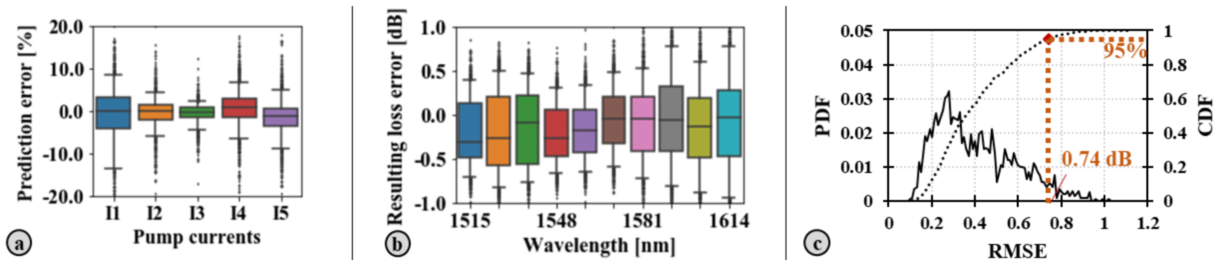

Fig. 3. Inverse model design results. (a) pump current prediction error repartition; (b) loss profile error repartition after remeasurement with predicted currents; (c): probability density function (PDF) of the RMSE and cumulative density function (CDF) of the RMSE

prediction error on the loss profile. We then compute the error between the initial profile and the re-measured loss. The loss error repartition is given in Fig. 3b: 90% of the examples show error less than ±0.9 dB, with 50% of the cases with ±0.6 dB error. The PDF and CDF of the RMSE are shown in Fig. 3c, showing good accuracy between target and re-measurement after current prediction, with mean RMSE of 0.41 dB, and 95% of predictions resulting in loss RMSE less than 0.74 dB. For this Raman design method, we attribute the worse performance compared to the *generative model* to the higher complexity of the prediction in the *inverse problem* and to the uncertainties of loss profile re-measurements after pump current predictions.

4. Application for multi-span transmission

In a multi-span experiment, we usually aim at setting the transmission line such that the power spectrum is identical at each span input, as shown in the inset 1 in Fig. 4a. With the power configuration described in our previous transmission work [4], we define our target loss as a linear profile with a tilt of 6 dB, yielding the power spectrum of the inset 2 of Fig. 4a at the next SOA input. We use the ANN of our design model to generate the corresponding pump current values, then measure the resulting loss profile and show the result in Fig. 3c (solid line). The measured loss profile shows good agreement with the target loss profile (dashed line), with limited ripples caused by multi-pump design, exhibiting a maximum error (vertical bars) of 1.52 dB and RMSE of 0.76 dB. Besides, improvement of our design method is expected from further optimization of the ANN architecture and learning parameters.

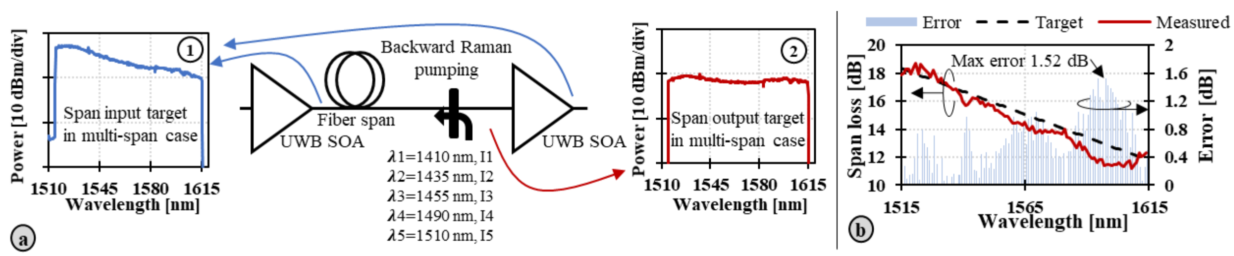

Fig. 4. (a): Power configuration for multi-span usage; (b): target, measured loss with currents given by ANN B prediction and resulting loss error

5. Conclusion

We reported on the experimental demonstration of the use of artificial neural networks to learn the mapping between Raman pump currents and UWB loss profile over a continuous 100 nm-wide optical spectrum in a 100 km-long SSMF span. On the one hand, our method can predict the loss profile given an arbitrary pump configuration. On the other hand, we achieve accurate pump configuration prediction not only for random loss profile but also to be able to meet a target loss profile. This method will be useful for the design of Raman amplifiers for multi-span ultra-wideband transmission systems.

References

[1] J. Renaudier, A. Ghazisaeidi, "Scaling Capacity Growth of Fiber-Optic Transmission Systems Using 100+ nm Ultra-Wideband Semiconductor Optical Amplifiers", in *J. Lightwave Technol.*, 37(8), pp. 1831-1838, 2019.

[2] F. Hamaoka, *et al.*, 'Ultra-Wideband WDM Transmission in S-, C-, and L-Bands Using Signal Power Optimization Scheme', in *J. Lightw. Technol.*, 37(8), 2019.

[3] M. Ionescu, *et al.*, '74.38 Tb/s Transmission Over 6300 km Single Mode Fiber with Hybrid EDFA/Raman amplifiers', in *Proc. OFC*, Tu3F.3, 2019

[4] A. Arnould, *et al.*, '103 nm Ultra-Wideband Hybrid Raman/SOA Transmission over 3×100 km SSMF', in *J. Lightw. Technol.*, Early Access, DOI: 10.1109/JLT.2019.2946590

[5] H. Kidorf, et al., 'Pump interactions in a 100-nm bandwidth Raman amplifier', in *IEEE Photonics Technology Letters*, 11(5), 1999.

[6] J. Zhou, *et al*, 'Robust, Compact, and Flexible Neural Model for a Fiber Raman Amplifier', in *J. Lightw. Technol*, 24(6), 2006.

[7] D. Zibar, *et al.*, 'Machine Learning-based Raman Amplifier Design', in *Proc. OFC*, M1J.1, 2019.

[8] A. M. R. Brusin, *et al*., 'An Ultra-Fast Method for Gain and Noise Prediction of Raman Amplifiers', in *Proc. ECOC*, Th.1.C.3, 2019.

[9] M. Ionescu, *et al*, 'Artificial Intelligence or Real Engineer, which is better ?', in *Proc. SubOptic 2019*.